Smart Structures and Systems, *Vol. 18, No. 1 (2016) 53-74*
DOI: http://dx.doi.org/10.12989/sss.2016.18.1.053

An experimental study on constructing MR secondary suspension for high-speed trains to improve lateral ride comfort

Y.Q. Ni[*1,2], S.Q. Ye[1] and S.D. Song[3]

[1]*Department of Civil and Environmental Engineering, The Hong Kong Polytechnic University, Hung Hom, Kowloon, Hong Kong*
[2]*Hong Kong Branch of National Rail Transit Electrification and Automation Engineering Technology Research Center, Hong Kong*
[3]*State Key Laboratory of Coastal and Offshore Engineering, Dalian University of Technology, Dalian 116023, China*

(Received September 26, 2015, Revised April 21, 2016, Accepted May 6, 2016)

Abstract. This paper presents an experimental study on constructing a tunable secondary suspension for high-speed trains using magneto-rheological fluid dampers (referred to as MR dampers hereafter), in the interest of improving lateral ride comfort. Two types of MR dampers (type-*A* and type-*B*) with different control ranges are designed and fabricated. The developed dampers are incorporated into a secondary suspension of a full-scale high-speed train carriage for rolling-vibration tests. The integrated rail vehicle runs at a series of speeds from 40 to 380 km/h and with different current inputs to the MR dampers. The dynamic performance of the two suspension systems and the ride comfort rating of the rail vehicle are evaluated using the accelerations measured during the tests. In this way, the effectiveness of the developed MR dampers for attenuating vibration is assessed. The type-*A* MR dampers function like a stiffness component, rather than an energy dissipative device, during the tests with different running speeds. While, the type-*B* MR dampers exhibit significant damping and high current input to the dampers may adversely affect the ride comfort. As part of an ongoing investigation on devising an effective MR secondary suspension for lateral vibration suppression, this preliminary study provides an insight into dynamic behavior of high-speed train secondary suspensions and unique full-scale experimental data for optimal design of MR dampers suitable for high-speed rail applications.

Keywords: high-speed train; lateral ride comfort; MR damper, secondary suspension; full-scale experiment

1. Introduction

The past decade has witnessed the tremendous development of high-speed rail in a number of countries. Today, high-speed rail becomes a part of highly efficient and economic public transport. Due to nonlinear wheel-rail interaction, however, high speed trains demonstrate diverse dynamic behaviors at different running speeds (Iwnicki 2006). In particular, when the trains operate at high speeds, the vibration responses of the vehicle that are induced by exterior inputs, mainly track

*Corresponding author, Professor, E-mail: yiqing.ni@polyu.edu.hk

http://www.techno-press.org/?journal=sss&subpage=8 ISSN: 1738-1584 (Print), 1738-1991 (Online)

irregularities, would be seriously aggravated, leading to problems pertaining to passenger ride comfort, vehicle stability and track maintenance. To address these problems, considerable efforts have been made to improve the vibration attenuation performance of rail vehicle suspensions. Most of the studies have been focused on primary suspension design that account for vertical vibration attenuation from track to bogie (Liao and Wang 2003, Mei and Goodall 2003, 2006). In general, secondary suspensions, which isolate the oscillation from bogie to car body, are more difficult in design, especially for lateral direction (Bruni *et al.* 2007). To improve the lateral ride comfort of high-speed rail vehicles, practical developments have tended to design secondary lateral suspensions.

There are three types of secondary lateral suspensions in general: passive, active, and semi-active suspensions. Currently, passive suspensions dominate the rail vehicle suspension market, since they are simple in design, reliable for implementation, and cost-effective. The passive suspensions are usually integrated with appropriately designed passive dampers (Fujimoto *et al*. 1996, Shieh *et al*. 2005). Their performance is solely dependent on the inherent dynamic characteristics of the system. In recent years, some innovative attempts have been made to enhance the dynamic performance. Jiang *et al*. (2012) incorporated inerters into a passive damper, so that the damper force is dependent not only on the velocity but also on the acceleration of the incorporated component. Despite advanced performance introduced, however, purely passive solutions are difficult to obtain dynamic performance encompassing high forward speeds and satisfactory ride comfort, etc.

As a counterpart, active suspension systems have been intensively studied over the past years (Oueslati *et al*. 1995, Bruni *et al*. 2007, Goodall 2011). The systems rely on transducers, actuators and active control laws to execute real-time vibration control of the vehicle. Active systems can achieve excellent control performance in a wide range of vehicle operation conditions. However, they are usually demanding in power supply and advanced actuators, which largely constrain the practical implementation in rail vehicle systems.

Semi-active suspension is an alternative to active suspension. It requires much lower power sources while it is capable of providing control performance comparable to its counterpart. In addition, the control performance is achieved by varying the damper dynamic characteristics, equivalently, by dissipating vibration energy, which in the active cases is obtained through energy input. A semi-active system enables not only fail-safe performance, but also preferable control performance. In a sense, it is the combination of passive and active control systems.

A main semi-active suspension is variable damping semi-active system. Stribersky *et al*. (1998) designed a semi-active damping system for rail vehicle secondary suspension, which consists of hydraulic dampers with continuously adjustable damping valve controlled by a skyhook controller. The suspension system can switch between two stages of characteristics, i.e., the soft and hard damping levels, in accordance with the car body velocity measured. An evaluation of the developed system showed great potentials in improving the ride comfort of the rail vehicle. Yang *et al*. (2006) designed a damper with multi-level damping, and developed adaptive fuzzy control using car body acceleration feedback to enhance the vibration attenuation capability of the suspension. Yang *et al*. (2011) studied the nonlinear feature of high-speed trains, and proposed a neural network based proportional integral derivative (PID) controller to accurately evaluate the damping force required. Zhao and Cao (2012) studied the lateral motions of a semi-active bogie with uncertain parameters. The result showed that the semi-active system had potentials to achieve the comfort standard set out by the active system. Incorporating MR dampers is another way to construct a semi-active secondary suspension. The MR dampers are able to vary their dynamic

characteristics in a wide range and response very fast by a driven voltage or current (Carlson *et al.* 1996, Spencer *et al.* 1997, Or *et al.* 2008, Yazid *et al.* 2014, Chen *et al.* 2015, El Wahed and Balkhoyor 2015). In addition, they have less demands in power supply, of mainly 12 V and 2 A, and installation space, which are two constraints in rail vehicle application. Several relevant investigations have recently been reported. Wang and Liao (2009a, b) studied the possibility of improving the lateral ride comfort of rail vehicle using MR secondary suspension. An LGQ vehicle controller and an MR damper controller were established, respectively. Their numerical simulations demonstrated an enhanced performance of the rail vehicle vibration attenuation under track irregularities input; however, oscillations of the bogies and wheels aggravated to some extent. Hudha *et al*. (2011) presented a preliminary study on vehicle-based skyhook and bogie-based skyhook control strategies for lateral secondary MR suspension.

Although MR secondary suspensions have great potentials for practical implementation in high-speed trains, it is still a new subject and needs to be explored in depth. So far, there have been only limited pioneering research works reported; and most of them were focusing on theoretical investigations and numerical simulations. This paper presents an experimental work on incorporating MR dampers in secondary suspensions in an effort to improve the lateral ride comfort of high-speed trains. The rail vehicles in tests are full-scale carriages of CRH3 electric multiple unit (EMU) high-speed train. Two types of MR dampers with different control ranges are designed, fabricated, and incorporated into the vehicle secondary suspensions. The integrated system runs on a roller rig under various speeds (40 to 380 km/h) with track irregularities input. Meanwhile, the performance of the MR suspensions is tuned by a driven current switching between passive-off and passive-on states. The dynamic behaviors of the integrated system at different control states, and the ride comfort of the rail vehicles are evaluated. This experimental study helps to determine the optimal state of MR secondary suspensions for a specified running speed level, and facilitates optimal design of MR dampers suitable for high-speed rail applications.

2. Experimental setup

2.1 High-speed EMU prototype for tests

This preliminary study is to experimentally verify the possibility of physically constructing MR secondary suspensions for lateral vibration attenuation of high-speed trains. The high speed rail vehicle used in tests is CRH3 EMU (Fig. 1). In the original secondary suspension, passive hydraulic dampers were equipped, linking the bogie and the carriage, for vibration suppression. In this study, two types of current-driven MR dampers (type-*A* and type-*B*) with different control ranges are designed, fabricated and incorporated to constitute MR secondary suspensions. The power supply of type-*A* MR dampers is 24 V and the maximum current input is 3.6 A. The maximum damper force of this type is up to 1,850 kN. The power supply of type-*B* MR dampers is 12 V and the maximum current input is 2 A. The dampers of this type are capable of providing a maximum control force of around 9 kN. Four MR dampers are incorporated in the secondary suspension, two in the leading bogie and the other two in the trailing bogie, replacing the passive hydraulic dampers in the lateral direction (Fig. 2). By tuning the current input through a linear voltage/current converter (VCC) (Fig. 3), the damping characteristics of the MR dampers would vary, and thus the dynamic performance of the secondary suspension would be adjusted accordingly. In this way, two MR secondary suspensions, simply System *A* (the secondary

suspension with type-*A* MR dampers) and System *B* (the secondary suspension with type-*B* MR dampers), are constructed.

Fig. 1 High-speed train prototype for tests

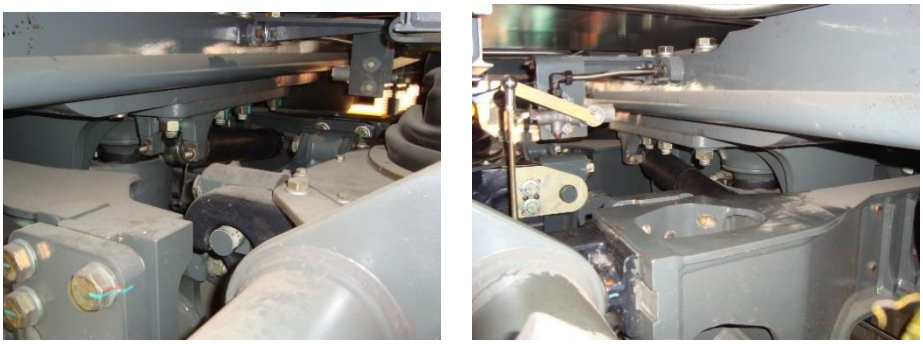

Fig. 2 MR dampers installed in secondary suspension

Fig. 3 Linear VCC

Fig. 4 Roller rig

The tests are conducted on a full-scale roller rig (Fig. 4) situated in the Traction Power State Key Laboratory of Southwest Jiaotong University, China. The EMU prototype runs on the roller rig at different speeds from 40 to 380 km/h with track irregularities. The longitudinal motion of the vehicle is constrained, and only the vertical and lateral oscillations are allowed. The spectrum of track irregularities, which was collected from the tracks of Guangzhou-Wuhan High-speed Rail Line in China, is imposed to the vehicle by executing vertical motions of the roller rig wheels. In doing so, actual dynamic behavior of the EMU prototype running on straight tracks is reproduced. The EMU prototype is tested without passengers-equivalent vehicle loading, because in practical operations the vehicle loading in general leads to lower natural frequency and consequently an even better ride comfort level is achieved (Iwnicki 2006).

During the experiments, sensors are installed to measure the dynamic behavior of the vehicle system tested. As shown in Fig. 5, accelerometers are mounted on the carriage floor (car body) and on the trailing bogie to measuring the vehicle acceleration in the lateral direction. The sensor sampling frequency is set to be 1,000 Hz. In this study, optical fiber accelerometers, rather than conventional electrical-type transducers, are employed. It is because there usually exist strong electromagnetic fields along high-speed rail lines and optical fiber sensors are immune to electromagnetic interference.

It should be noted that the nonlinearity stemming from wheel-rail contact usually leads to diverse dynamic responses of a rail vehicle system under different forward speeds. As a result, the vibration behavior relates strongly to the operation speed (Iwnicki 2006, Cheli and Corradi 2011). It is therefore reasonable to determine the optimal status of the MR suspension for each speed level. For simple and practical implementation, the MR secondary suspension can be designed to function between several states that are solely dependent on current input to the incorporated dampers. In this study, current input to the installed MR dampers is adjusted from 0 A to the allowable maximum at each running speed, and at the meantime the dynamic behavior of the vehicle and the ride comfort are evaluated. Thus, the tests are conducted enable to determine the optimal current input with best ride comfort for a specified running speed. In return, the designed MR dampers could be judged on their applicability to the EMU prototype tested. System *A* is tested first, and then followed by System *B*.

(a) Accelerometer on car body (b) Accelerometer on bogie

Fig. 5 Optical fiber accelerometers deployed

2.2 Rolling-vibration tests on System A

Four type-*A* MR dampers (Fig. 6) are used in the secondary suspension of the vehicle, accounting for lateral vibration attenuation of the carriage. Fig. 7 shows the dynamic hysteresis behaviors of type-*A* MR dampers at a frequency of 5 Hz with an amplitude of 10 mm for current inputs I = 0, 0.5, 1.0 and 1.5 A, respectively, which were measured by displacement-controlled experiments of an individual damper on an MTS test system. The hysteresis loops have been obtained under different frequencies, amplitudes and current inputs.

In the rolling-vibration tests, the four MR dampers are connected to a linear VCC by the wired cables. The tests on the integrated system are conducted at ten standard service speeds, i.e., 40, 80, 120, 160, 200, 250, 280, 320, 350 and 380 km/h. For each speed level, the current input (I) of the four MR dampers is simultaneously adjusted from 0 A to the allowable maximum 3.6 A in eight stages, that is, 0, 0.5, 1.0, 1.5, 2.0, 2.5, 3.0 and 3.6 A. With the change in current input, the dynamic performance of the MR suspension varies accordingly.

Fig. 6 Type-*A* MR dampers

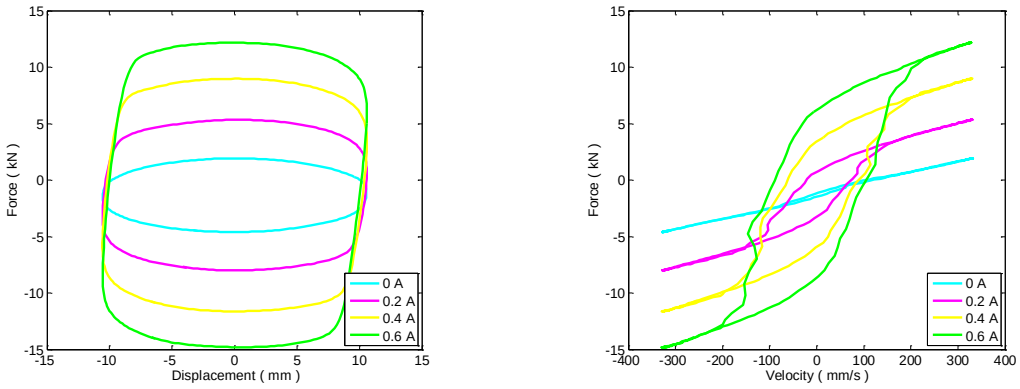

(a) Force-displacement hysteresis loops (b) Force-velocity hysteresis loops

Fig. 7 Dynamic hysteresis behaviors of type-*A* MR dampers

2.3 Rolling-vibration tests on System B

Rolling-vibration tests are then followed on the integrated System *B*. Similarly, four type-*B* MR dampers (Fig. 8) replace the original passive dampers connecting the bogies and the carriage in the lateral direction, two in the leading truck and the other two in the trailing truck, constructing a tunable MR suspension. The power supply of type-*B* dampers is 12 V, and the maximum current input is 2 A. Fig. 9 illustrates the dynamic hysteresis behaviors of type-*B* MR dampers at a frequency of 5 Hz with an amplitude of 10 mm for current inputs I = 0, 0.2, 0.4 and 0.6 A, respectively. It is found that the saturation current of type-*B* MR dampers is about 1.4 A. In the rolling-vibration tests, the vehicle runs on the roller rig at seven speeds, namely, 120, 160, 200, 250, 280, 320 and 350 km/h. The experiment is stopped at a running speed of 350 km/h because large vibrations are observed at this speed. For each service speed, the dynamic performance of the MR suspension is captured by switching the current input (I) to 0, 0.2, 0.4, 0.6, 0.8, 1.0, 1.2 and 1.4 A, respectively.

Fig. 8 Type-*B* MR dampers

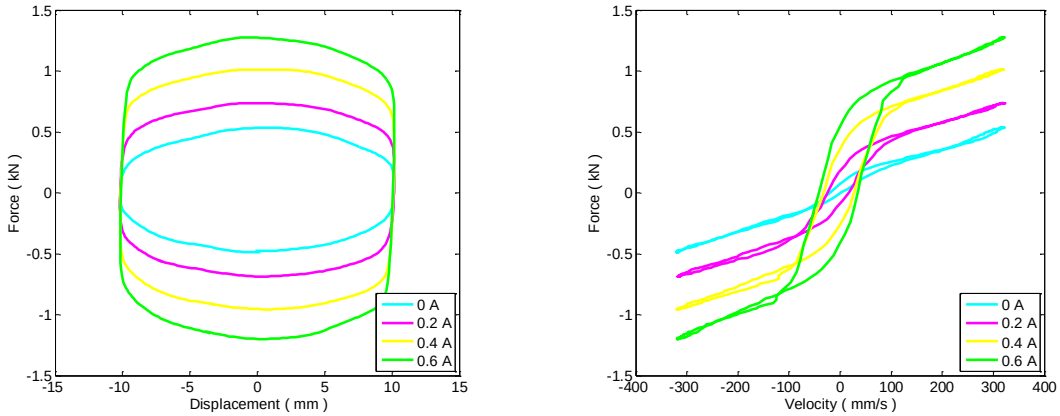

(a) Force-displacement hysteresis loops (b) Force-velocity hysteresis loops

Fig. 9 Dynamic hysteresis behaviors of type-*B* MR dampers

3. Ride comfort index

The simplified formula for evaluating passenger ride comfort stipulated in UIC Code 513 (1994) is used to quantify the vibration level of the carriage and assess the dynamic performance of the MR suspensions under different operation conditions. Since this study focuses on the effect of laterally-deployed MR dampers on transverse motions of the rail vehicle, only the lateral component of the comfort index is calculated. With the obtained ride comfort index, the effectiveness of the dampers on attenuating the vibration can be determined for each specific current input.

The lateral component of the ride comfort index is obtained by

$$N_{MV} = 6\left|a_{YP95}^{W_d}\right| \tag{1}$$

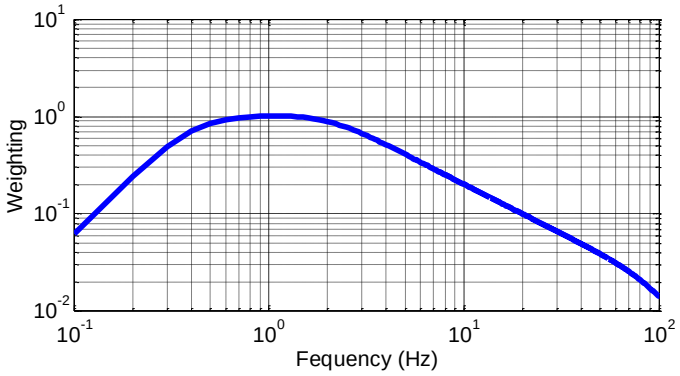

Fig. 10 Frequency weighting filter W_d

where a_Y denotes accelerations measured at floor level of a carriage in the lateral direction. The superscript W_d refers to a frequency weighting filter which is given in Fig. 10. The filter is applied to the measured accelerations to obtain the frequency-weighted accelerations. The subscript *P95* represents the 95 percentile effective value, which is calculated every 5 seconds. Smaller the index value is obtained, better ride experience is indicated. In the present study, the lateral component (rating) of the ride comfort index equal to 1 is considered as an acceptable comfort level. It is worth noting that the dynamic response components in the frequency range of 0.4 to 5.0 Hz, especially between 0.6 and 2.0 Hz, contribute considerably to the lateral comfort index. Therefore, attenuation of vibrations in this frequency region would be the key to optimal state of the constructed MR suspension.

4. Results and discussion

4.1 Rolling-vibration tests on System A

The rolling-vibration tests on System *A* are conducted at 10 running speeds from 40 to 380 km/h, with current input to the four type-*A* MR dampers being simultaneously tuned from 0 to 3.6 A. It is observed that when the running speed is increased to 160 km/h, the lateral vibration of the vehicle becomes unstable when the current input is tuned to 1.0 A, which is signaled by a clearly visible periodic motion. Fig. 11 shows a comparison of car body motions in stable condition (I = 0.5 A) and in unstable condition (I = 1.0 A) at running speed of 160 km/h. Resonant vibration at 1.9 Hz is excited when the current input is increased to 1 A. The lateral vibration amplitude of the car body rises considerably to 1.5 m/s^2, compared with 0.5 m/s^2 when the current input is 0.5 A. When the running speed is further increased to 200 km/h, the instability of vibration occurs as the current input is equal to 0.5 A. It implies that the type-*A* MR dampers with current input are too stiff for the vehicle when the running speed exceeds 200 km/h. As a result, the remaining tests for higher running speeds are conducted only at damper passive-off state with null current input.

The measured accelerations of the car body in the lateral direction are analyzed to obtain the ride comfort rating. The accelerations are filtered with a band pass filter in the frequency range of 0.4 to 80.0 Hz, and then weighted to calculate the UIC ride comfort index according to Eq. (1). The resulting rating is plotted in Fig. 12. The zero values in the figure refer to the cases where rolling-vibration test was not conducted due to the potentially unstable oscillation.

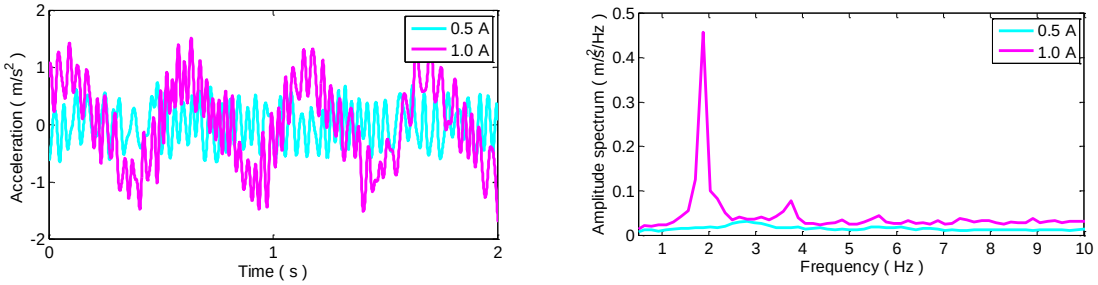

(a) Acceleration time history (b) Acceleration amplitude spectrum

Fig. 11 Lateral vibration of car body at running speed of 160 km/h

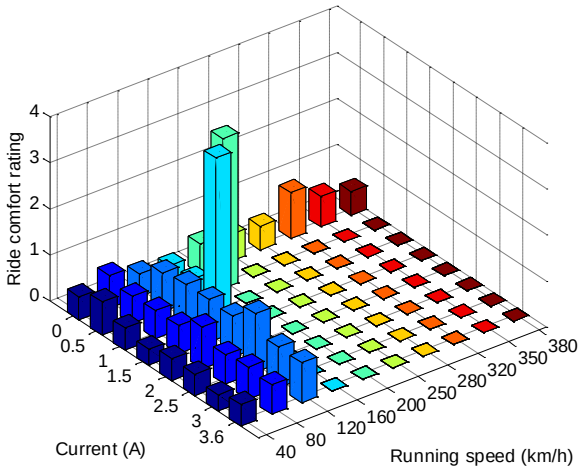

Fig. 12 Ride comfort rating of power (motor) car tested

As illustrated in Fig. 13, the car body demonstrates different ride comfort rating under different running speeds at damper passive-off state. Fig. 14 shows the lateral acceleration amplitude spectra at running speeds of 80, 200 and 320 km/h, respectively. It can be seen that there is no dominant mode governing the car body vibration. Instead, the car body undergoes forced vibration in a wide frequency range. In the case of 80 km/h running speed, the car body exhibits much vibration in the frequency range of 0.6 to 2.0 Hz, causing a less comfortable ride. In the case of 200 km/h running speed, high-frequency components are slightly intensified. However, low-frequency components, especially in the frequency range around 2.0 Hz, are attenuated, leading to a slight improvement of the comfort rating. When the running speed is equal to 320 km/h, the car body experiences large vibration in the frequency range around 2.8 Hz and in the higher frequency range, and therefore a degraded ride condition is achieved. Obviously, the running speed has a strong influence on the dynamic behavior of the vehicle. In view of the fact that human body is extremely sensitive to motions in the frequency range of 0.4 to 5.0 Hz, the optimal state of the MR suspension should be tuned to a level that effectively suppresses these frequency components. And this solution would favorably contribute to the improvement of the passenger ride comfort.

In the case of low running speeds (40 km/h and 80 km/h), the vehicle demonstrates generally satisfactory ride comfort rating (lower than 0.7) under different current inputs. At running speed of 40 km/h, the rating is 0.5 at passive-off state, and degrades to 0.7 as the current input is tuned to 0.5 A, and then keeps around 0.5 at the subsequent passive-on states. Fig. 15 shows the acceleration amplitude spectra of the car body at speed of 40 km/h with current inputs of 0 and 0.5 A, respectively. It is observed that the vibration patterns are similar, both in broadband responses. With the increase of current input, the oscillation amplifies in both low and high frequency regions, resulting in a degradation of comfort rating. When the vehicle runs at 80 km/h, the rating is

generally around 0.67. The maximum (worst) one happens at the current input of 2 A. A comparison of the acceleration amplitude spectra is shown in Fig. 16, which also reveals an increase of vibration in both low and high frequency regions. For a higher speed at 120 km/h, the best comfort rating is about 0.5 which occurs at damper passive-off state. As current input increases, the rating degrades to around 0.9. It reaches a peak value of about 1.3 at the current input of 2.5 A. Fig. 17 shows the acceleration amplitude spectra of the car body at running speed of 120 km/h. It is observed that with the increase of current input from 0 to 1.0 A, the response components over the whole frequency range are amplified.

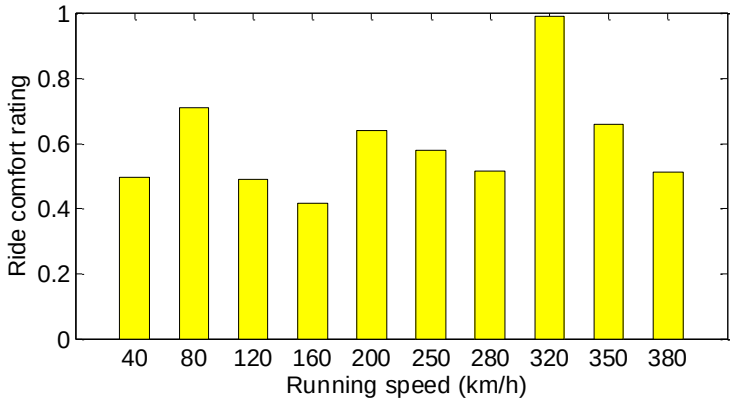

Fig. 13 Ride comfort rating at damper passive-off state

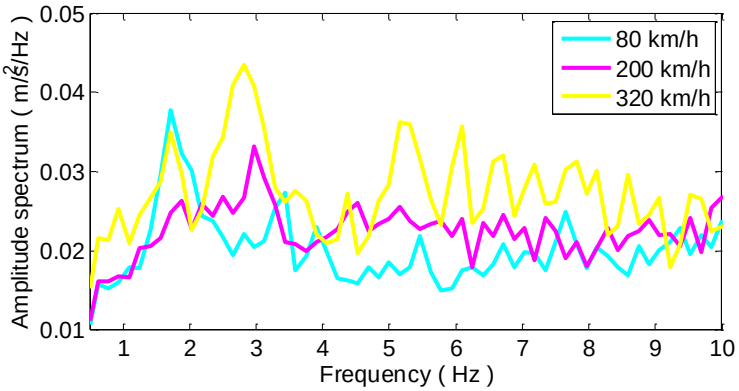

Fig. 14 Amplitude spectrum of lateral acceleration of car body at damper passive-off state

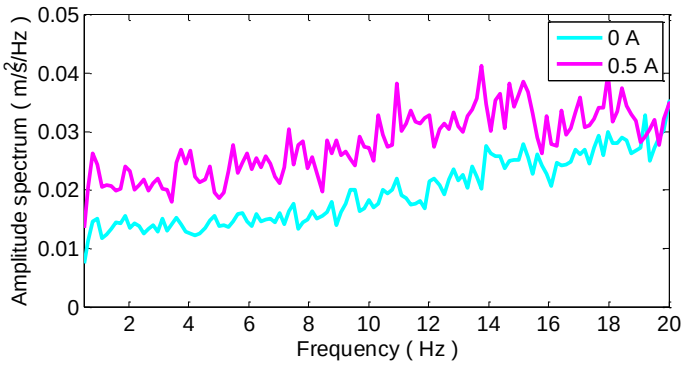

Fig. 15 Amplitude spectrum of lateral acceleration of car body at running speed of 40 km/h

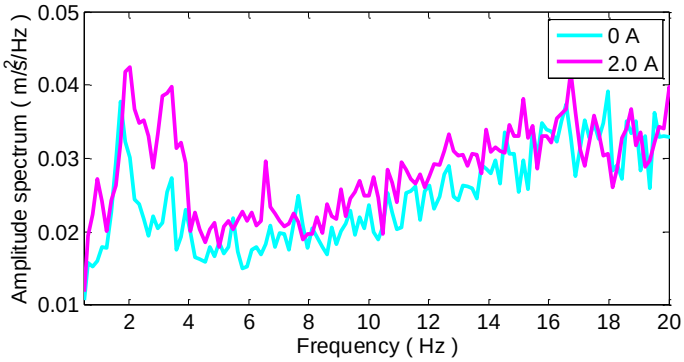

Fig. 16 Amplitude spectrum of lateral acceleration of car body at running speed of 80 km/h

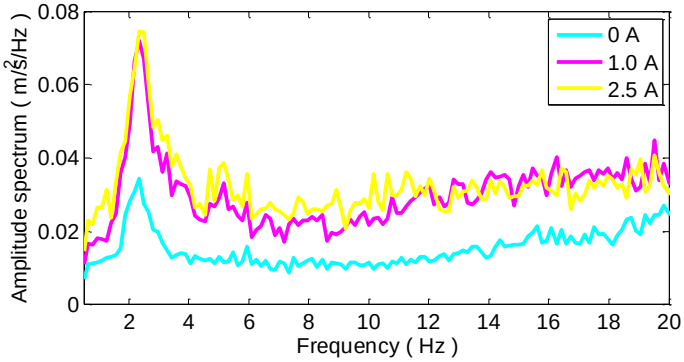

Fig. 17 Amplitude spectrum of lateral acceleration of car body at running speed of 120 km/h

Since there is a potential of instability in oscillation with further increasing running speed, only limited experimental data are collected to assess the dynamic performance of System *A*. In general, the dynamic response characteristics of the car body in both low and high frequency regions vary with the change of current input. However, the classic trade-off between resonant vibration and higher-frequency oscillation is not observed when changing the current input. It is probably due to small relative motions between the bogies and the carriage as we observed during the tests. In this case, the MR dampers are likely to perform as stiffness components, or even joints, to transfer vibration energy from bogies to car body, rather than to dissipate energy. This would lead to a degraded ride comfort. In conclusion, the type-*A* MR dampers are too stiff, making them effective only in the situation of low running speeds.

4.2 Rolling-vibration tests on System B

The rolling-vibration tests on System *B* are then conducted at seven running speeds from 120 to 350 km/h. The maximum operation load of the type-*B* MR dampers is around 9 kN. For each speed level, the current input to the four MR dampers is tuned synchronously from 0 to 1.4 A at intervals of 0.2 A. The ride comfort rating is calculated using the measured lateral accelerations of the car body in each test. Fig. 18 shows the lateral ride comfort rating of the car body obtained at different running speeds with various current inputs. The vehicle generally demonstrates stable dynamic behaviors with the ride comfort rating below 1.2 when the running speed doesn't exceed 320 km/h. When the speed reaches 350 km/h, however, considerably large vibration of the vehicle is observed, and a substantial deterioration of comfort degree is obtained. Therefore, the rolling-vibration tests stop at this speed level.

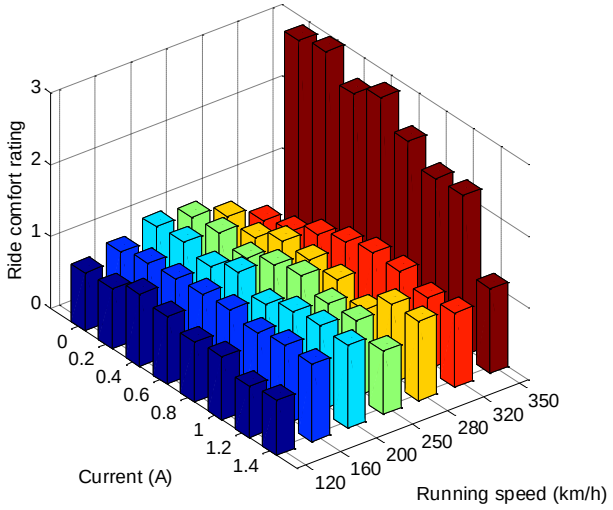

Fig. 18 Ride comfort rating of trailer car tested

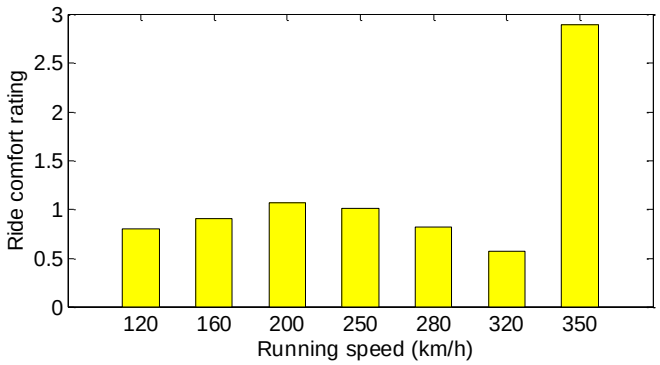

Fig. 19 Ride comfort rating at damper passive-off state

Fig. 19 illustrates the lateral ride comfort rating of the car body under different speed levels at damper passive-off state. Compared with System *A*, System *B* demonstrates favorable attenuation of vibration at running speed of 320 km/h though it turns poor at 350 km/h. Fig. 20 shows the lateral acceleration amplitude spectra of the car body under different running speeds. It is observed that in all the cases, broadband responses rather than dominant modal vibrations are excited. As the vehicle speeds up to 200 km/h, low-frequency vibration components become larger, resulting in a slight degradation in ride comfort. At running speed of 320 km/h, the vehicle vibrates less in low-frequency region but more in high-frequency region. Because the comfort rating is more sensitive to low-frequency components, a satisfactory rating is obtained. When the vehicle accelerates to 350 km/h, however, a substantial increase of vibration is observed. The secondary suspension with type-*B* MR dampers at passive-off state is incompetent to suppress the lateral vibration of the vehicle when the running speed exceeds 350 km/h.

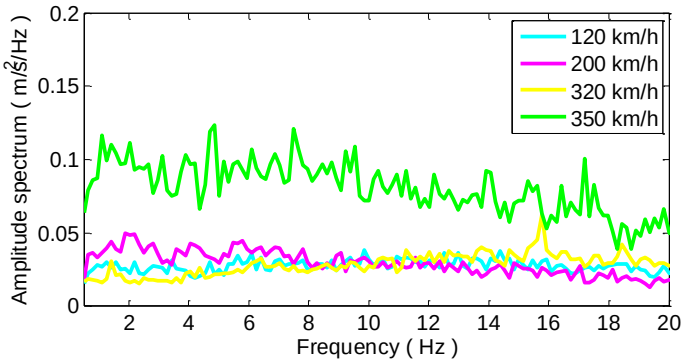

Fig. 20 Amplitude spectrum of lateral acceleration of car body at damper passive-off state

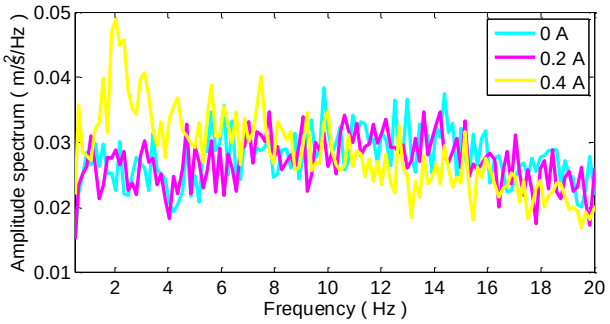

Fig. 21 Amplitude spectrum of lateral acceleration of car body at running speed of 120 km/h

When the running speed is between 120 and 280 km/h, the ride comfort of the vehicle exhibits variations in a narrow range when imposing different current inputs. For example, the ride comfort rating varies between about 1.0 and 1.2 at running speed of 200 km/h. It is interesting to note that with increasing current input, energy transmission between low and high frequency regions occurs. At running speed of 120 km/h, the vibration components at low-frequency range are amplified as the current input is increased to 0.4 A (Fig. 21). When the running speed is 160 km/h, low-frequency vibration components are excited at the current input equal to 0.2 A (Fig. 22). Since the ride comfort is sensitive to low-frequency region, especially in the frequency range of 0.4 to 5.0 Hz, the increased low-frequency response results in a degradation in comfort degree. As the vehicle accelerates to 250 km/h, on the other hand, resonant vibration is attenuated when the current input is 0.4 A (Fig. 23), resulting in an improvement of the comfort rating. In general, improvement or deterioration of the ride comfort rating is compliant with attenuation or amplification of resonant oscillations. Although the vehicle exhibits diverse dynamic behaviors at running speeds between 120 and 280 km/h, satisfactory comfort rating can be achieved with the current input between 0 and 0.4 A.

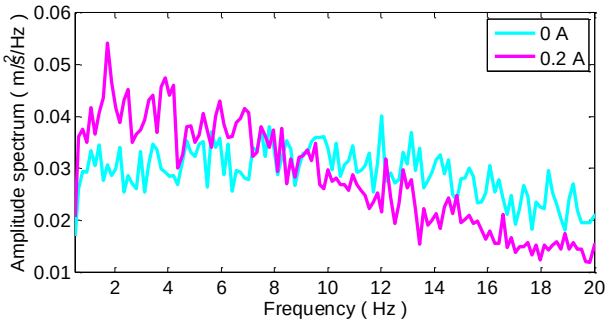

Fig. 22 Amplitude spectrum of lateral acceleration of car body at running speed of 160 km/h

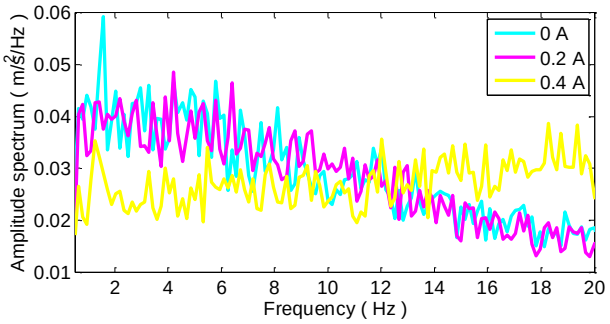

Fig. 23 Amplitude spectrum of lateral acceleration of car body at running speed of 250 km/h

When the running speed comes to 320 km/h, the comfort rating exhibits a rather obvious trend in terms of current input. The optimal working condition is observed at damper passive-off state, at which the comfort rating is 0.5. With the increase of current input, the rating degrades at its onset and reaches its maximum (worst) value at 0.8 A, and then improves slightly when the current input is further increased (Fig. 24). Fig. 25 shows the lateral acceleration amplitude spectra of the car body. At passive-off state, the low-frequency vibration components of the car body are quite small. When current input is imposed, however, the vibration components in the frequency range of 0 to 8.0 Hz aggravate significantly, leading to a reduction in comfort degree.

Because the vibration of the car body is transmitted from the bogie by connecting components such as dampers and springs, it is reasonable to examine the dynamic behavior of the bogie such that the performance of the lateral suspension system can be further assessed. A statistical analysis method (Mantaras and Luque 2006) is applied herein to evaluate the measured acceleration of the vehicle bogie. The root mean square (RMS) of the acceleration response at the bogie is calculated every 1 second. Then the 95 percentile value is selected to characterize the bogie dynamics.

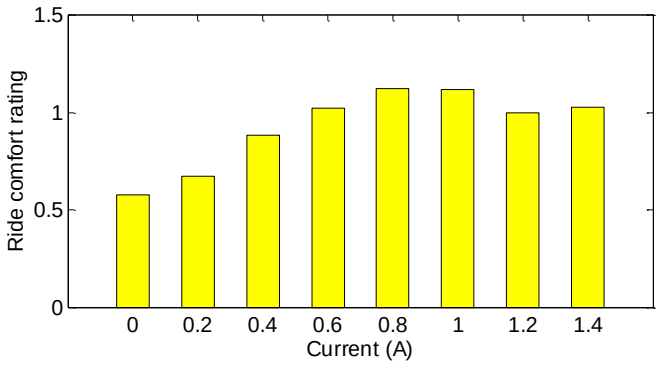

Fig. 24 Ride comfort rating at speed of 320 km/h

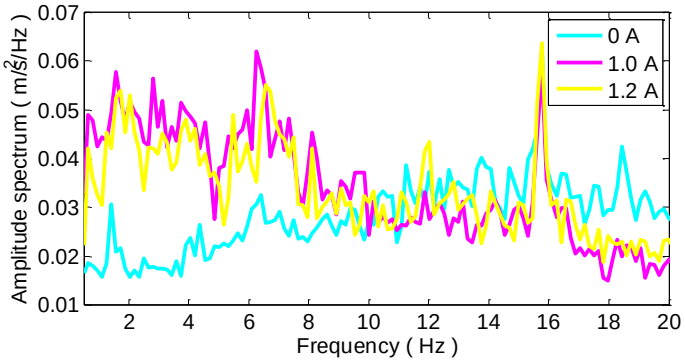

Fig. 25 Amplitude spectrum of lateral acceleration of car body at speed of 320 km/h

The resulting statistical histogram at running speed of 320 km/h is presented in Fig. 26. It can be seen that when changing the current input, the effective acceleration of the bogie varies slightly from 0.36 m/s^2 at passive-off state to 0.4 m/s^2 at passive-on state with the current input of 1.4 A. It indicates that the vibrations of the car body (carriage) and the bogie are relatively independent. The lateral acceleration amplitude spectra of the bogie at the same running speed are illustrated in Fig. 27. Consistent with the observed effective acceleration of the bogie, the response spectra exhibit only minor fluctuations over the whole frequency range under different current inputs. No substantial variation is observed in the frequency-domain response. The passive-off state with null current input gives rise to the smallest bogie acceleration.

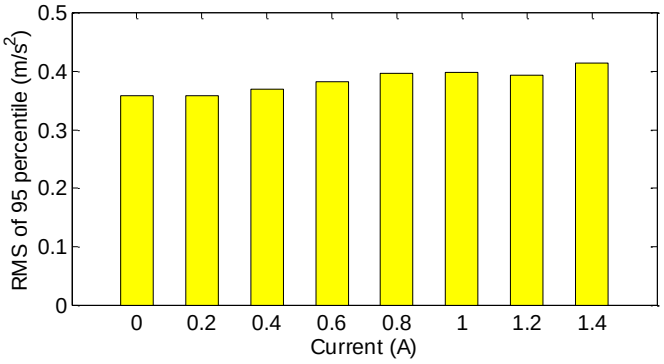

Fig. 26 95 percentile of RMS values of bogie lateral acceleration at speed of 320 km/h

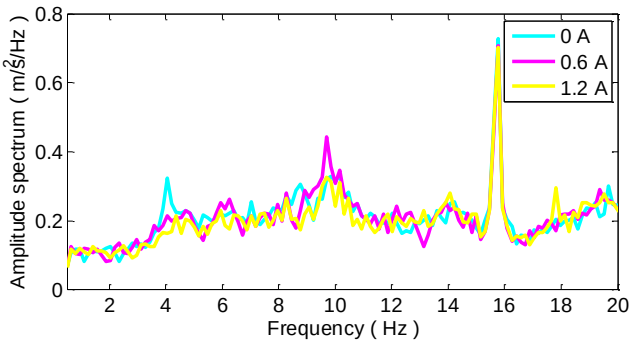

Fig. 27 Amplitude spectrum of lateral acceleration of bogie at speed of 320 km/h

When the vehicle running speed is 350 km/h and the MR dampers are at passive-off state, the car body exhibits serious vibration. The comfort rating is evaluated to be 2.9 (Fig. 28), indicating a very uncomfortable ride status. As current input increases, a general decrease of the comfort rating is observed, and the minimum (best) value is achieved with the current input of 1.4 A. Since the saturation current of the dampers is around 1.4 A, the tests are stopped at this current input. The lateral acceleration amplitude spectra of the car body at running speed of 350 km/h are shown in Fig. 29, in which a considerable variation of the frequency-domain response with changing current input is observed. At damper passive-off state, low-frequency components are dominant in the lateral vibration of the car body. When the current increases to 0.6 A, a trade-off between low-frequency oscillation aggravation and high-frequency vibration suppression is attained. Owing to a higher weighting of low-frequency oscillation in evaluating the ride comfort rating, a slight decrease (improvement) in the comfort rating is obtained. When the current input is tuned to 1.0 A, the response components in the frequency range of 0 to 10.0 Hz are further suppressed, resulting in a reduction in the comfort rating. When the current input is finally increased to 1.4 A, low-frequency oscillations are attenuated while high-frequency response components keep almost the same as in the case of 1.0 A. Consequently the comfort rating is improved to be 1.2.

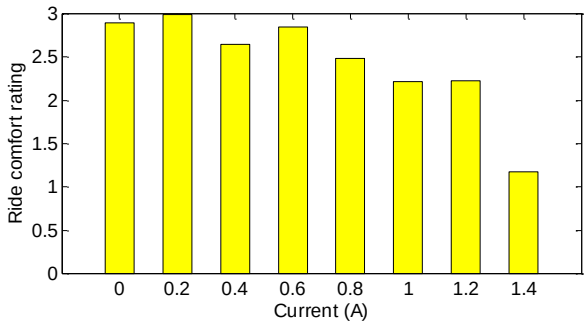

Fig. 28 Ride comfort rating at speed of 350 km/h

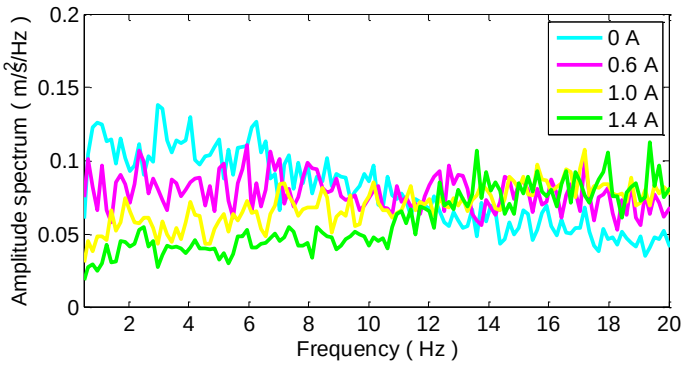

Fig. 29 Amplitude spectrum of lateral acceleration of car body at speed of 350 km/h

The acceleration of the bogie at vehicle running speed of 350 km/h is also evaluated. Figs. 30 and 31 show the dynamic behavior of the bogie at this running speed, including the 95 percentile RMS response and acceleration amplitude spectra. Compared to the bogie vibration at 320 km/h, the effective acceleration of the bogie becomes larger, but is still less affected by changing current input. Again, the vibrations of the bogie and the car body are relatively independent, indicating insignificant transmission of vibration energy between the two parties. It is therefore inferred that the vibration energy of the car body is dissipative primarily by the MR dampers when turning the current input. Because the MR secondary suspension at passive-off state results in considerably large vibration of the car body when the vehicle running speed exceeds 350 km/h, MR dampers with lower adjustable damping forces would be more appropriate for high-speed rail applications.

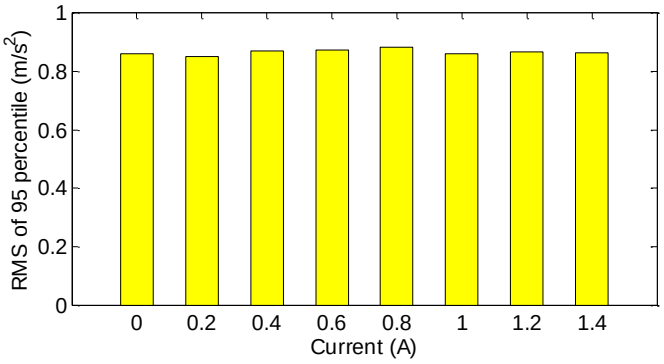

Fig. 30 95 percentile of RMS values of bogie lateral acceleration at speed of 350 km/h

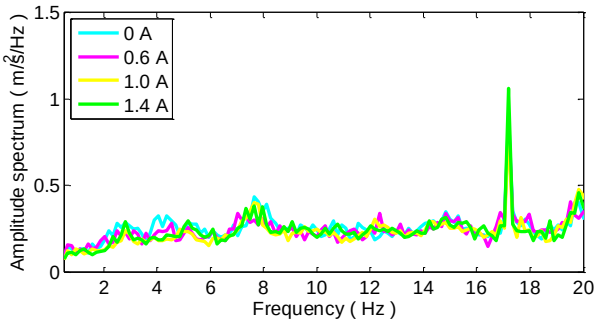

Fig. 31 Amplitude spectrum of lateral acceleration of bogie at speed of 350 km/h

5. Conclusions

As part of an ongoing investigation on developing MR secondary suspension for ride comfort improvement of high-speed trains, this study presented an experimental study of two MR secondary suspensions. Two types of MR dampers (type-*A* and type-*B*) with different control ranges were designed, manufactured and incorporated into rail secondary suspension for lateral vibration attenuation of rail car bodies. Full-scale high-speed rail vehicles using the developed MR secondary suspensions were tested on a roller rig with running speeds from 40 to 380 km/h and input of track irregularities spectrum collected from a high speed rail line. With the measured dynamic responses, ride comfort rating of the car body tested was calculated to evaluate the dynamic performance of the two MR secondary suspensions.

From the rolling-vibration tests, it is found that the secondary suspension incorporating type-*A* MR dampers is favorable only when the vehicle running speed is relatively low. When the running speed is equal to or higher than160 km/h, the lateral vibration of the car body tends to be unstable when the current input attains a certain level. In such situations, the car body vibration is sensitive to change in the current input. Because of small relative motions between the bogie and the carriage, the MR dampers perform like a stiffness component to transfer vibration energy from bogie to car body without significant energy dissipation. In conclusion, the type-*A* MR dampers are too stiff for suppressing lateral vibration of rail vehicles when running at high speeds.

The secondary suspension incorporating type-*B* MR dampers exhibit better energy dissipation capacity. The optimal state of the MR suspension (optimal current input to MR dampers) with best ride comfort of the car body has been obtained for each running speed level in concern. It is observed that the suppression of low-frequency response components is greatly beneficial to improving the ride comfort. With appropriate current input, a trade-off between low-frequency oscillation and high-frequency vibration can be achieved, verifying the effectiveness of the MR secondary suspension in adjusting the damper force. However, the secondary suspension with type-*B* MR dampers at passive-off state is incapable of suppressing the lateral vibration of the vehicle when the running speed exceeds 350 km/h. In recognizing this, new MR dampers with more appropriate adjustable damping forces are currently being developed to construct more effective MR secondary suspensions.

Acknowledgments

The work described in this paper was supported in part by the National Science Foundation of China under Grant No. U1234210, and partially by a grant from the Innovation and Technology Commission of the Hong Kong SAR Government to the Hong Kong Branch of National Rail Transit Electrification and Automation Engineering Technology Research Center. The authors are also obliged to the technical support provided by Lord Corporation, USA.

References

Bruni, S., Goodall, R., Mei, T.X. and Tsunashima, H. (2007), "Control and monitoring for railway vehicle dynamics", *Vehicle Syst. Dyn.*, **45**(7-8), 743-779.

Carlson, J.D., Catanzarite, D.M. and St. Clair, K.A. (1996), "Commercial magneto-rheological fluid devices", *Int. J. Modern Phys. B*, **10**(23-24), 2857-2865.

Cheli, F. and Corradi, R. (2011), "On rail vehicle vibrations induced by track unevenness analysis of the excitation mechanism", *J. Sound Vib.*, **330**(15), 3744-3765.

Chen, Z.H., Ni, Y.Q. and Or, S.W. (2015), "Characterization and modeling of a self-sensing MR damper under harmonic loading", *Smart Struct. Syst.*, **15**(4), 1103-1120.

El Wahed, A.K. and Balkhoyor, L.B. (2015), "Magnetorheological fluids subjected to tension, compression, and oscillatory squeeze input", *Smart Struct. Syst.*, **16**(5), 961-980.

Fujimoto, H. and Miyamoto, M. (1996), "Lateral vibration and its decreasing measure of a Shinkansen train (decrease of train vibration with yaw damper between cars)", *Vehicle Syst. Dyn.*, **25**(1), 188-199.

Goodall, R.M. (2011), "Control for railways active suspensions and other opportunities", *Proceedings of the 19th Mediterranean Conference on Control and Automation*, Corfu, Greece.

Hudha, K., Hafiz Harun, M., Hanif Harun, M. and Jamaluddin, H. (2011), "Lateral suspension control of railway vehicle using semi-active magnetorheological damper", *Proceedings of the IEEE Intelligent Vehicle Symposium (IV)*, Baden-Baden Germany.

Iwnicki, S. (ed.) (2006), *Handbook of Railway Vehicle Dynamics*, Taylor & Francis, Boca Raton, FL, USA.

Jiang, J.Z., Matomoros-Sanchez, A.Z., Goodall, R.M. and Smith, M.C. (2012), "Passive suspensions incorporating inerters for railway vehicles", *Vehicle Syst. Dyn.*, **50**(1), 263-276.

Liao, W.H. and Wang, D.H. (2003), "Semiactive vibration control of train suspension systems via magnetorheological dampers", *J. Intell. Mat. Syst. Str.*, **14**(3), 161-172.

Mantaras, D.A. and Luque, P. (2006), "Ride comfort performance of different active suspension systems", *Int. J. Vehicle Des.*, **40**(1-3), 106-125.

Mei, T.X. and Goodall, R.M. (2003), "Recent development in active steering of railway vehicles", *Vehicle Syst. Dyn.*, **39**(6), 415-436.

Mei, T.X. and Goodall, R.M. (2006), "Stability control of railway bogies using absolute stiffness: sky-hook spring approach", *Vehicle Syst. Dyn.*, **44**(l), 83-92.

Or, S.W., Duan, Y.F., Ni, Y.Q., Chen, Z.H. and Lam, K.H. (2008), "Development of magnetorheological dampers with embedded piezoelectric force sensors for structural vibration control", *J. Intell. Mat. Syst. Str.*, **19**(11), 1327-1338.

Oueslati, F., Rakheja, S. and Sankar, S. (1995), "Study of an active suspension for improved ride quality and reduced dynamic wheel loads", *Road Transport Technol.*, **4**, 441-452.

Shieh, N.C., Lin, C.L., Lin, Y.C. and Liang, K.Z. (2005), "Optimal design for passive suspension of a light rail vehicle using constrained multiobjective evolutionary search", *J. Sound Vib.*, **285**(1-2), 407-424.

Spencer Jr., B.F., Dyke, S.J., Sain, M.K. and Carlson, J.D. (1997), "Phenomenological model of magnetorheological damper", *J. Eng. Mech. - ASCE*, **123**(3), 230-238.

Stribersky, A., Kienberger, A., Wagner, G. and Muller, H. (1998), "Design and evaluation of a semi-active

damping system for rail vehicles", *Vehicle Syst. Dyn.*, **29**(1), 669-681.
Wang, D.H. and Liao, W.H. (2009a), "Semi-active suspension systems for railway vehicles using magnetorheological dampers. Part I: system integration and modeling", *Vehicle Syst. Dyn.*, **47**(11), 1305-1325.
Wang, D.H. and Liao, W.H. (2009b), "Semi-active suspension systems for railway vehicles using magnetorheological dampers. Part II: simulation and analysis", *Vehicle Syst. Dyn.*, **47**(12), 1439-1471.
Yang, J., Li, J. and Du, Y. (2006), "Adaptive fuzzy control of lateral semi-active suspension for high-speed railway vehicle", *Proceedings of the International Conference on Intelligent Computing*, Kunming, China.
Yang, Z., Zhang, B., Zhang, J. and Wang, C. (2011), "Research on semi-active control of high-speed railway vehicle based on neural network-PID control", *Proceeding of the 7th International Conference on Natural Computation*, Shanghai, China.
Yazid, I.I.M., Mazlan, S.A., Kikuchi, T., Zamzuri, H. and Imaduddin, F. (2014), "Magnetic circuit optimization in designing Magnetorheological damper", *Smart Struct. Syst.*, **14**(5), 869-881.
Zhao, N. and Cao, D.Q. (2012), "Semi-active control and its robustness for a bogie model with uncertain parameters", *Proceeding of the 1st International Workshop on High-Speed and Intercity Railways*, Hong Kong.